EFDA–JET–PR(10)11

A. Semerok, S.V. Fomichev, F. Brygo, P.-Y. Thro, C. Grisolia
and JET EFDA contributors

Pulsed Repetition Rate Nanosecond Laser Heating and Ablation of the Tokamak Graphite Tile Deposited Layers

Pulsed Repetition Rate Nanosecond Laser Heating and Ablation of the Tokamak Graphite Tile Deposited Layers

A. Semerok[1], S.V. Fomichev[1], F. Brygo[1], P.-Y. Thro[1], C. Grisolia[2]
and JET EFDA contributors*

JET-EFDA, Culham Science Centre, OX14 3DB, Abingdon, UK

[1]CEA Saclay, DEN/DPC/SCP/LILM, Bat. 467, 91191 Gif-sur-Yvette, France
[2]CEA Cadarache, DSM/IRFM, 13108 Saint-Paul-lez-Durance, France
** See annex of F. Romanelli et al, "Overview of JET Results",*
(Proc. 22 [nd] IAEA Fusion Energy Conference, Geneva, Switzerland (2008)).

Preprint of Paper to be submitted for publication in
Journal of Nuclear Materials

ABSTRACT.
Laser heating and ablation of plasma-facing surface of graphite tile from TEXTOR tokamak with a deposited carbon layer were under study. Laser heating measurements were performed with a pulsed nanosecond Nd-YAG laser (2^{nd} harmonic, 10kHz repetition rate, 100ns pulse duration). Surface temperature measurements were made with the developed pyrometer system. The experimental results were simulated with the theoretical model of laser heating of a surface with a deposited layer by periodically repeating laser pulses. The comparative experimental and theoretical study of the laser heating temperature traces allowed to characterise the deposited carbon layer if thermal and optical properties of the graphite substrate are known. Laser ablation measurements were made with two pulsed nanosecond Nd-YAG lasers (20Hz and 10kHz repetition rate with 5ns and 100ns pulse duration, respectively). For the plasma-facing graphite surface with a thick (~30-50μm) deposited carbon layer, the ablation threshold was 0.45±0.1 J/cm^2 without dependence on the applied pulse duration. The obtained ablation threshold was significantly lower than the one for the backside non-plasma-facing surface of tokamak graphite without a carbon deposit. The comparison of the experimental and theoretical results demonstrated that the laser ablation mechanisms for tokamak graphite and thick carbon layers deposited on plasma-facing surface are different.

1. INTRODUCTION

Deposited carbon layer formation with excessive tritium trapping in tokamak plasma-facing surfaces is regarded as a severe problem for efficient operation of thermonuclear D-T fusion reactors [1-7]. Laser Heating (LH) [8-12] and laser ablation (LA) [13-18] may be suggested to provide an efficient tritium inventory control. LH was applied to release hydrogen isotopes from the deposited layer and to measure hydrogen concentration [19] rather than to remove the carbon deposit from the surface. LA with a high repetition rate (10-20kHz) by commercially available powerful (10-100W mean power) pulsed nanosecond Nd-YAG lasers may be suggested for cleaning and detritiation of tokamak internal walls by removing the carbon deposited layers from plasma-facing components [20-24]. In this case, an optimised sucking system should be provided in order not to increase the in vessel dust inventory. Laser beam transportation by an optical fiber allows both to remove the laser system away from the contaminated zone and to perform remote surface treatment [25].

To avoid graphite tile damage during the deposited layer removal, LA thresholds both for graphite and carbon layers should be known. LA threshold and rate of the carbon deposit depend both on the deposited layer properties (thickness, density, thermal and optical features, adhesion with the substrate) and those of the graphite substrate. To our knowledge, these properties are not sufficiently known. The thermal and optical layer properties may differ significantly from those of tokamak graphite. To obtain the graphite and layer properties, the thermal response of the corresponding surface to the transient heat pulse should be measured [26].

The experimental and theoretical results on LH and LA of the backside (non-plasma-facing)

surface of graphite tiles from Tore Supra tokamak (CEA Cadarache, France) to characterise some thermal and optical properties of manufactured tokamak graphite were under comparative study within the developed simulation model [27].

This paper presents the LH and LA results for a graphite plasma-facing surface with a carbon deposited layer from TEXTOR tokamak (Garching, Germany). This study should be regarded as a continuation of our investigations on the tokamak graphite without deposit [27]. The tile sample from the toroidal belt pump limiter (ALT-II tile prepared from isotropic graphite Toyo Tanso, IG-430U) was under study. The preliminary results on comparative experimental and theoretical studies were presented in [28]. In this paper, Chapter 2 presents the experimental and simulation results on LH of plasma-facing surface with a deposited carbon layer on different zones of TEXTOR graphite tile. For LH study with laser-active pyrometer measurements, a high repetition rate laser (10 kHz repetition rate, 100 ns pulse duration, 532 nm wavelength) combined with the developed pyrometer system was applied. To determine the deposited layer properties, theoretical fit of the experimental temperature traces was made. On the TEXTOR tile, different zones with different layer thickness and adhesion with the graphite substrate were analyzed. Chapter 3 presents the experimental and simulation results on LA of the same sample. For a thick carbon layer (~30-50 μm) deposited on the TEXTOR graphite tile, the LA threshold was much lower than the one for a pure graphite surface without dependence on the applied pulse duration (5 ns or 100 ns). The contaminated surface cleaning could be provided without graphite substrate damage. LA rate of the layer was found to be much higher than the one for pure graphite surface. It may be attributed to rather different LA mechanisms for graphite and thick deposited layers. The conclusions are given in Chapter 4.

2. LASER HEATING MEASUREMENTS & THE DEPOSITED LAYER CHARACTERISATION

2.1. EXPERIMENTAL RESULTS.

In our studies, LH was provided by a Nd-YAG laser (2^{nd} harmonic, 10kHz repetition rate, 100ns laser pulses, up to 50 W mean power). The experimental pyrometer system based on a single-color Impac-Kleiber C-LWL infra-red pyrometer (600-2600K temperature range, 1.6-2.2μm working wavelength range, 15 μs response time ($t_{99\%}$)) was developed. The laser fluence of a homogenized ("top hat") laser beam on the surface was $F \approx 0.3 J/cm^2$ with the laser pulse energy $E_p = 6MJ$ and about 1.5 mm laser spot diameter. The experiments were performed on graphite tiles from the TEXTOR belt pump limiter (ALT-II tile) with a deposited carbon layer. Fig.1 presents the tile zones under study with different deposited layer properties (thickness, friability, adhesion). Fig.2 presents the LH pyrometer measurements results on these zones. Hereafter (in Figs. 2-9) the heating temperature (in K) means the difference between the sample temperature measured by pyrometer and the environment (room) temperature.

In Figure 2 (panels a-i), the visually determined layer quality is in agreement with the gradual modification of the temperature traces. In Fig.2 (panels a-b), the LH traces are quite similar. They correspond, respectively, to the zone without the deposited layer and the zone with a layer, but

deeply ablated by 10 laser scans1, i.e., to a pure graphite surface with bulk graphite properties. Both temperature traces reveal a slow increase of the pre-heating temperature (due to the heat accumulation with high repetition rate LH). However, as the pre-heating temperature did not exceed the bottom temperature limit of the pyrometer (at least, during LH time with 150 laser pulses), it was not possible to compare accurately the results of these measurements with the calculations. But they are in a good qualitative agreement with the bulk graphite properties specified in [27] (see Chapter 2.2). The experimental/calculation results comparison was easier for a very thin deposited layer (Fig.2, panel c) as the pre-heating temperatures were very close to the bottom temperature limit of the pyrometer at the end of LH with 100 pulses. Thus, to estimate the layer properties, it was possible to compare the experimental/calculations results both for the pre-heating temperature and the temperature profile between two adjacent laser pulses.

In Figure 2 (panels d, e, f), the LH temperature traces with the pre-heating temperature well above the bottom threshold of the pyrometer are presented. In panels (e) and (f), the pre-heating temperature is very stable beginning with the 20^{th} and 30^{th} laser pulse, respectively. The experimental LH temperature stability is often observed for high heating peak temperatures. It may be associated with inaccuracy of the pyrometer temperature measurements when the peak heating temperatures are close to or higher than the top temperature limit of the pyrometer due to saturation of the pyrometer photocurrent. Thus, only the initial part of the LH traces is suitable for the experimental/calculation results comparison. These cases are very similar to LH of a backside surface of Tore Supra graphite tile [27], where the experimental pre-heating temperatures stabilisation was also observed.

In Figure 2 (panels g, h, i), the experimental results correspond to a rather thick deposited layer. From Fig.2 (g), these results are very reproducible and two different measurements (with different LH time) performed in the same tile zone are well superimposed. However, from Fig. 2 (g) and also Fig. 2 (h, i), the top temperature limit of the pyrometer was exceeded already with 30 laser pulses. This conclusion was based on pre-heating temperature saturation in this time range and also on cutting the experimental results for the peak heating temperatures corresponding to the top temperature limit of the pyrometer. In all these cases, the heating temperature increased very quickly, and it was very high already for 30 laser pulses. However, the temperature decrease (when the laser was off) depends on the tile zone. It may be associated either with a different layer thickness or adhesion. Thus, LH measurements demonstrated that high repetition rate LH temperature traces depend strongly on the deposited layer properties.

2.2. LH MODELLING AND THE LAYER PROPERTIES

To simulate LH of a deposited carbon layer, both thermal properties of a graphite substrate and thermal and optical features of the layer should be known. The layer thickness and adhesion with the substrate should be also known. The adhesion quality corresponds to the thermal resistance of

[1]In this zone, LA was performed by Nd-YAG laser (20kHz repetition rate, 250μm laser spot diameter on the surface, 2J/cm^2 laser fluence). The scanning velocity was 0.5m/s. Thus, one laser scan corresponded to ten laser pulses on a given surface zone.

the layer/substrate interface, which is the proportionality coefficient between the heat flow through the interface and the temperature jump on two interface sides. Generally, as these features for carbon deposited layers are not well known, LH simulations with the mean temperature-independent thermal and optical layer features (between room temperature $T_0 = 300$K and graphite sublimation temperature $T_S = 4200$K) are required. Modelling of high repetition rate LH was applied to tokamak graphite [27] and to paint and industrial cement [29]. In our modelling, it was assumed that the layer substance is the same tokamak graphite sputtered from the graphite wall eroded due to hightemperature plasma heating in the working tokamak and then re-deposited with some density (which may be different from the bulk graphite density). Some layer features (volume specific heat c_L, laser absorption coefficient α_L and reflectivity coefficient R_L) can be estimated through the corresponding reference graphite properties c_0, α_0 , R_0 and carbon layer porosity p_L . The linear dependence on density for the volume specific heat, laser absorption coefficient and the refractive index can be applied with sufficient accuracy. The porosity of the tile graphite in nuclear industry is about 25% [30, 31]. The mean tokamak graphite properties specified in [27] are as follows: the mean volume specific heat is $c_G = 2.5$ MJ/(m3 K) , the mean laser absorption coefficient $\alpha_G = 2$ μm-1, the mean reflectivity $R_G = 0.22$ and the mean thermal conductivity coefficient $k_G = 60$ W/(m K). Fig. 3 presents the calculations of LH of tokamak graphite surface (without the layer) with the above thermal and optical features for laser fluence $F \approx 0.3$ J/cm^2. For comparison, Fig.3 presents also the experimental results for the tile zone, where the deposited layer was completely removed by LA (Fig.2 (b)). In this case, the pre-heating temperature was lower than the bottom temperature limit of the pyrometer. Thus, the quantitative comparison of the experimental/calculations results is not possible. However, the experimental results both for the graphite surface without the carbon deposits and for the surface where the deposited layer was completely removed by LA (panel (a) and panel (b) of Fig.2, respectively) are in a qualitative agreement with the calculations on LH for the pure tokamak graphite surface. For both cases, the exceeding of the calculated peak heating temperatures with respect to the experimental ones is associated with averaging the actual heating temperatures over a long response time ($t_{99\%} = 15$μs) of the pyrometer (about 100 times longer than 100 ns laser pulse duration).

For LH simulations with the deposited carbon layer on a graphite surface, the layer porosity p_L, the layer thermal conductivity k_L, the thermal resistance of the layer/substrate interface h and the layer thickness d remain as adjusting properties, which should be defined from the LH calculation/ experimental results fitting. However, for thin layers ($d \sim 1$μm), to determine simultaneously both the layer thickness and porosity seems to be a problem [27]. The thermal properties of the layer are defined by its total heat capacity (proportional to $(1-p_L)d$). For thin deposited layers, it is reasonable to assume that the layer porosity is not high, at least not exceeding the 25% porosity of the bulk graphite. Even a lower porosity can be assumed, taking into account the sputtering and atomization of the graphite under high-temperature plasma in operating tokamaks.

Thus, for thin deposited layers, the LH simulations were performed with assumed $p_L = 0$. Fig.4

presents the LH simulation results for a thin carbon layer deposited on the TEXTOR tile. The experimental temperature trace from panel (c) of Fig.2 is visually similar to those on panels (a) and (b) of Fig.2 and corresponds to the cases without a carbon deposit, except for the end of LH when the heating temperature is very close to the bottom temperature limit of the pyrometer. A good fit of the experimental results was made with the following layer properties: $p_L = 0$, $d = 5\mu m$, $k_L = 0.7 W/(m\ K)$, $h = 250 kW/(m^2\ K)$, thus indicating that the adhesion between the thin layer and the substrate is good. However, the thermal conductivity of the layer is low (much lower than the thermal conductivity of tokamak graphite). The simulation results are in a good agreement with the experimental results not only for the whole temperature trace (pre-heating temperatures), but also for cooling curves between two adjacent laser pulses. The microsecond response time of the pyrometer was not the only reason to omit the peak heating temperatures from the fitting with the calculated ones. The other important reason was the essential dependence of the peak heating temperatures on the laser absorption coefficient of the deposited layer, assuming that it could be an additional adjusting property. However, the pre-heating temperature profile does not depend practically on the laser absorption coefficient of the layer, which affects only the peak heating temperatures. For the qualitative agreement with the calculations, the experimental peak temperatures should be lower than the calculated peak heating temperatures due to averaging on the 15 microsecond response time of the pyrometer.

The LH simulation results for the temperature trace from panel (d) of Fig.2 are presented in Fig.5. This zone on the graphite tile with a carbon deposit was ablated by one laser scan, so some residual deposit can be present. A good agreement between the experimental and calculation results (both for the whole pre-heating profile and the cooling curve between two adjacent pulses) was obtained for the following layer properties: $p_L = 0$, $d = 1.7\mu m$, $k_L = 0.4\ W/(m\ K)$, $h = 60 kW/(m^2\ K)$. The initial layer thickness in this zone on the TEXTOR tile was much higher (of the order of a few tens of microns). The simulation results show that LA by one laser scan has almost removed the deposited layer from the graphite surface, leaving only a residual layer of a few microns. The thermal conductivity of a residual layer is of the same order as for a thin deposited layer, but the adhesion with a substrate is worse. Instability of the experimental pre-heating temperatures may be attributed to the ablated area inhomogeneity.

Figure 6 presents the LH simulations results for the temperature trace from panel (e) of Fig.2. This zone on the tile with a carbon deposit corresponds to a thin deposited layer. The fit was made for the initial laser heating. The extreme stability of the experimental pre-heating temperatures could be an artifact attributed to either the pyrometer (saturation of the pyrometer photocurrent at the temperatures close to and above the top temperature limit of the pyrometer) or to abnormal heating regime of graphite layer. A good agreement between the experimental and calculations results (both for the whole profile and the cooling curve between two adjacent laser pulses) was obtained for the following layer properties: $p_L = 0$, $d = 3.8\mu m$, $k_L = 0.2 W/(m\ K)$, $h = 100 kW/(m^2\ K)$. Though the heating temperatures were higher (if compared with the case of Fig.4), the layer thickness

waslower. The thermal conductivity was lower. The layer/substrate adhesion was also worse.

From Figure 7, where LH simulations were made for the temperature trace from panel (f) of Fig.2, the LH temperatures are two times higher than for the traces in Fig.5 and Fig.6. The fit was performed with the initial LH temperatures. A good agreement between the experimental and calculations results was obtained for the following layer properties: $p_L = 0$, $d = 10\mu m$, $k_L = 0.4$ W/(m K), $h = 60 kW/(m^2 K)$. In accordance with the visual observations, the layer thickness was higher than in all the previous cases, but both the thermal conductivity and the layer/substrate adhesion were of the same order, respectively.

Due to the uncertainty in the layer porosity, some uncertainty remains in the layer thickness estimations. But assuming $p_L = 25\%$ (as for the bulk tokamak graphite), the estimated layer thickness could be only 30% higher if compared with the case of $p_L = 0$. Thus, for thin layers lower than or of the order of ten microns in thickness (for which, probably, the expected layer porosity does not exceed the porosity of the bulk graphite), the layer thickness and other layer properties may be estimated with a sufficiently good accuracy.

For thick layers, it was also not possible to determine unambiguously the layer porosity and thickness. For thick deposited layers (estimated by the optical microscope as a few tens of microns in thickness), the layer porosity was expected to be higher than the reference bulk graphite porosity (25 %). Fig. 8 presents the LH simulation results for different assumed layer thickness as compared with the experimental temperature trace from panel (h) of Fig.2. A good fit (including both the LH period and the temperature relaxation curve after LH was off) can be obtained for different layer thickness[2] (from 11.5μm with $p_L = 0$ up to 50μm with $p_L = 69\%$). The increase of the pre-heating temperatures is defined mainly by pL, but the slope of the relaxation curve tail (when the laser is off) is defined mainly by the heat transfer coefficient h. The LH temperature scale is defined by the layer thermal conductivity k_L (at a given laser fluence F). The dependences of three adjusting properties on the assumed layer thickness are shown in panel (d) of Fig.8. As it was expected, the layer porosity p_L undergoes the largest variation versus the layer thickness (approximately under the law $(1- p_L) \sim d^{-1}$).

As a good fit of the experimental results can be achieved in a wide range of assumed layer thickness, the layer density should be known to estimate accurately the layer thickness from these measurements. Or, vice versa, one should know the layer thickness to estimate the layer porosity. The thick layer thickness on TEXTOR tile in these zones was measured independently by optical microscopy as being 30–50μm. For the case of Fig.8, it corresponds to 50–70% layer porosity. With the assumed 50% layer porosity, the layer thickness in the zone corresponding to Fig.8 may be deduced as being approximately 30μm. The thermal conductivity and adhesion were not very sensitive to the layer thickness. Although the layer thermal conductivity was of the same order as for thin layers (of the order of a few tens of W/(m K)), the adhesion of a thick layer with a substrate was much worse ($h \approx 3$ kW/(m^2 K) for the case of Fig.8).

[2]*Note that it turns out impossible to fit perfectly the final part of LH, where the peak heating temperatures exceed the top temperature limit of the pyrometer. In this range, the pyrometer measurements reliability is under the question.*

The similar analysis was made for the results presented in Fig.9 corresponding to the zone on the TEXTOR tile very close to that of Fig. 8. However, the layer properties were different. The adhesion with a substrate was worse because $h \approx 1$ kW/(m^2 K). This correlates with different behavior of the temperature relaxation curves when LH is off. The reasonable layer porosity $p_L = 50\%$ corresponds to a higher layer thickness of ≈40μm. The thermal conductivity is $k_L \approx 0.2$W/(mK) (approximately the same). The results obtained indicate that the comparative study of different zones on the surface with the deposited carbon layer is possible. However, independent measurements of the layer density or thickness for layer properties characterisation are required.

For thin and thick deposited carbon layers, the layer thermal conductivity was very low if compared with the one of the tokamak graphite. It may be attributed to a high content (≈50%) of hydrogen isotopes in the TEXTOR tile deposited layer [5, 21]. The low thermal conductivity allows to estimate layer properties by fast calculations in 1-D approximation. In this case, these calculations are relevant due to a strongly suppressed radial heat transport. The results obtained with 1-D simulations and those with significantly longer 3-D calculations were almost the same. The layer properties estimation was also made for the case presented in panel (g) of Fig.2. For the assumed 50% layer porosity, a good fit corresponds to the following layer properties: $d = 19$μm, $k_L = 0.14$ W/(m K), $h = 11$kW/(m^2 K), indicating that in this tile zone, the layer is thinner than for the cases of Fig.8 and Fig.9. The adhesion is better, as one can see from the faster decrease of the temperature relaxation curve. The thermal conductivity is of the same order. However, the saturation of the experimental pre-heating temperature profile (where the peak temperature is high enough) is far from being in a complete calculation/experimental results agreement. To explain these experimental results, further investigations on nanosecond LH pyrometer measurements are required.

3. LA OF DEPOSITED CARBON LAYERS

3.1. EXPERIMENTAL RESULTS

TEXTOR tokamak graphite sample with a thick (30-50μm) deposited carbon layer was under LA study. The LA experimental results were obtained with two Nd-YAG lasers (532nm wavelength, 20Hz low repetition rate, 5ns laser pulses and 10kHz high repetition rate, 100ns laser pulses) on the same sample which was under LH measurements with the pyrometer (Fig.1). The experimental results on the zone under LA are presented in Fig.10. For 5ns laser pulses, different laser fluences were obtained by varying the laser pulse energy at the fixed laser spot diameter (1mm). For 100ns laser pulses, different laser fluences were obtained at the constant laser pulse energy (6mJ), but by varying the laser spot diameter. From Fig.10, no significant difference in both LA threshold and rate for these two cases is observed. For both cases, the LA thresholds are about 0.45 J/cm^2, which is significantly lower than the corresponding ablation thresholds (1 J/cm^2 for 5ns laser pulses and 2.5 J/cm^2 for 100ns pulses) of tokamak graphite [27]. This difference in LA thresholds for tokamak graphite and a thick deposited layer, especially for 100ns pulses, can be applied to ensure selfcontrol of laser cleaning of tokamak graphite walls.

Near the LA threshold, the experimental crater depth H (per laser pulse) can be described by a linear function of the laser fluence up to 1J/cm^2. So, in this range

$$H \approx \beta (F - F_{th}) \quad (1)$$

with $\beta \approx 0.3\mu m \times cm^2/J$ (the slope of dot lines in Fig.10). This value is ten times higher than the one obtained for the backside (non-plasma-facing) surface of graphite sample from Tore Supra [27]. It means that LA efficiency is much higher for a thick carbon deposited layer than for pure graphite. For LA of a thick deposited layer, the same LA threshold for 5ns and 100ns laser pulses could be attributed to the decrease in both light absorption and thermal conductivity of the layer if compared with bulk graphite. Thus, even for 100ns laser pulses, LH depth is comparable with or lower than the laser beam absorption length.

For the case corresponding to Fig.10, the crater depth was approximately a linear function of a number of applied laser shots both for short and long pulse durations (as for tokamak graphite [27]). For 5ns laser pulses at 20Hz repetition rate, the linear dependence of the crater depth on the number of applied laser pulses was expected. In contrast, for 100ns laser pulses at 10kHz repetition rate, the linear dependence would be quite unexpected, taking into account the considerable heat accumulation from pulse to pulse (see Fig.2, panels (g), (h) and (i)). However, as the experimental results in Fig.10 were obtained by averaging the LA rate over a large number of applied laser pulses (up to 1000 pulses very near LA threshold and about 100 pulses for higher laser fluences), the conclusion about practical identity of the LA thresholds and rates for both cases may be considered valid only on the average.

The important conclusion about the layer LA mechanism may be deduced if the experimental LA rate and the maximal theoretical LA rate are compared within the framework of surface sublimation/vaporisation mechanism shown in Fig.10 by a thick line. It is described by the equation [32] :

$$H \approx (1-RL)\,(F - F\text{th})/L\,\text{r}L \quad (2)$$

L =50MJ/kg is the latent mass sublimation specific heat of graphite. The assumed layer porosity p_L is 50%, which corresponds to the layer thickness d = 30-40μm in our LH simulations (Fig.8 and Fig.9). As seen from the comparison, the experimental LA rate is above the maximal theoretical LA rate by the surface sublimation mechanism, thus indicating that the surface sublimation (vaporisation) can not describe LA of a thick deposited layer. Further modifications and improvements of laser ablation model [27] are required for an adequate description of the deposited layer ablation by nanosecond pulses.

3.2. SIMULATION OF LA EXPERIMENTAL RESULTS AND THEIR INTERPRETATION

The Stefan-like sublimation model of LA is relevant to describe the experimental results on nearthreshold LA of tokamak graphite by nanosecond laser pulses [27]. This model involves the

standard heat equation with the Stefan boundary condition [32] on the moving external ablation front due to surface sublimation/ vaporisation. With the specified graphite properties, both calculated LA thresholds and rates were in a good quantitative agreement with the corresponding experimental results for 5ns (532nm) laser pulses of 20Hz repetition rate and for 100ns (532nm) pulses of 20Hz and 10kHz repetition rates.

The simulation results of deposited carbon layer LA obtained with this model both for 5 ns and 100ns laser pulses are presented in Fig.11 (curves 1 and 2). The layer thermal and optical properties and the heat transfer coefficient h through the layer/substrate interface were taken from LH simulations presented in Fig.9 (d) with the assumed layer thickness $d = 40$ μm on the TEXTOR tile. The other layer properties were taken as follows: $p_L = 53\%$, $k_L = 0.18$ W/(m K), $h = 1.15$kW/(m^2 K).

The ablation rates (crater depths) were obtained for a single laser pulse of a respective duration without allowance for any pre-heating effect. Thus, for periodically repeating laser pulses, they can be strictly relevant only for a sufficiently low repetition rate (for 5ns pulses in our study). For both 5ns and 100ns pulse durations, a practically complete identity of the calculation results was obtained. A slight difference between them is only near the LA threshold, which was 0.6J/cm^2 for both cases. This value (obtained without any additional adjustments) may be regarded as being in a good correspondence with the experimental LA threshold for a thick carbon layer deposited on tokamak graphite tile.

However, the LA depth calculated with the layer surface sublimation mechanism of LA (superimposed curves 1 and 2 in Fig.11) is much lower than the experimental one. It is also much lower than the probable maximum LA depth (Eq.2), which can be reached within the framework of the layer sublimation mechanism (Fig.10). This discrepancy may be due to a sufficiently low layer thermal conductivity, which essentially reduces the reverse flux of the thermal energy to the external layer surface. It also reduces the surface sublimation/ vaporisation and the velocity of LA front. Thus, the layer surface sublimation mechanism can hardly be responsible for the experimentally measured LA depth. However, a good agreement in LA thresholds indicates that the thermal model of LA (in which the sublimation temperature is of importance) could be applicable with some modifications.

In Figure 12, the calculated surface sublimation depth is presented as a function of time for 5ns laser pulse at different laser fluences F. The calculations show that the time of the active surface sublimation of the layer is generally much longer than the laser pulse duration. For F > 0.7J/cm^2, this time is longer than 100ns. The similar results were obtained for 100ns pulses. The calculations demonstrate that the time of the laser pulse action is of insignificant contribution to the whole surface ablation depth. The main contribution may be attributed to the times when the laser pulse is off. Thus, the actual time of surface sublimation of the layer $t$subl is much longer than 5ns and 100ns laser pulse durations in our investigations.

During the time t_{subl}, the layer overheating above the sublimation temperature T_s at some distance inside the layer takes place (in accordance with the Stefan boundary condition). The calculated

overheating depth as a function of laser fluence is presented in Fig.11 (curves 3 and 4). The overheating depths for two different pulse durations are almost the same. This overheating depth corresponds to the heat penetration depth inside the layer $(k_L t_{subl}/c_L)^{1/2}$ on a time scale of $t$subl.

The overheating depth is approximately 2-3 times higher than the experimental ablation depth. The experimental ablation depth is more than ten times higher than the one calculated within the surface sublimation mechanism of LA. Thus, the overheating depth is at least in a semi-quantitative agreement with the experimental LA depth. If the experimental LA depth is of the order of the overheating depth, the LA mechanism of the thick deposited carbon layer can be qualitatively close to the so-called explosive mechanism of LA [33]. In our case, it may be associated with a high porosity of a thick deposited layer if compared with bulk graphite and, as a consequence, with a lower mechanical breaking strength of the layer. When the layer is overheated above the sublimation temperature, the intensive volume sublimation takes place inside the layer pores and cavities. Due to the induced inner pressure and the low breaking strength of the layer substance, the layer is removed from the depth of the order of overheating depth. Thus, the ablated matter may be considered not only as a completely atomized layer, but rather as a mixture of layer atoms with solid particles and liquid droplets. It was confirmed by our preliminary studies on micro-particle size distribution for graphite and deposited layer LA with high repetition rate nanosecond lasers.

The effect of high repetition rate (10kHz) on LA efficiency may be expected as the essential dependence of the LA threshold on the number of applied laser pulses. The calculated LA threshold dependence (obtained with LH results of Fig.9) is presented in Fig.13. For the first laser pulse (no pre-heating), the LA threshold is about 0.6J/cm^2. For the 100th laser pulse, it decreases down to 0.15J/cm^2. As the experimental crater depth (per one laser pulse) for 100ns laser pulses of 10kHz repetition rate were obtained with averaging over several laser pulses (up to 100), the experimental/calculation results agreement on a single-shot basis may be regarded as satisfactory. For deeper understanding both LH and LA of a thick deposited layer, further experimental studies are required for extracting the dependence of LA thresholds and rates on the number of applied laser pulses of a high repetition rate.

CONCLUSIONS

Our investigations were aimed to study LH and LA of plasma-facing surface of graphite tile from TEXTOR tokamak with a deposited carbon layer of a different thickness.

LH measurements were performed with a pulsed nanosecond Nd-YAG laser (2nd harmonic, 10kHz repetition rate, 100ns pulse duration). Surface temperature measurements were made with the 10μs time resolution by the pyrometer system. The experimental results were simulated with the developed theoretical model of LH of a surface with the deposited layer by periodically repeating laser pulses. A good agreement was obtained between the LH experimental/theoretical results. The theoretical fit of the experimental temperature profiles obtained with the pyrometer measurements allowed to obtain some unknown properties of the deposited layer to provide layer characterisation.

With some reasonable value of layer porosity p_L, three properties (heat transfer coefficient h, layer thickness d, and layer thermal conductivity k_L) can be determined from the experimental/simulated results fitting. For a porous deposited carbon layer, the layer thickness can be unambiguously determined only if the layer density is known, and the layer density can be defined only if the layer thickness is known[3]. Thus, the comparative experimental and theoretical study of the LH temperature traces allowed to characterise the deposited carbon layer if thermal properties of the graphite substrate were known.

LA measurements were made with two pulsed nanosecond Nd-YAG lasers (2nd harmonic, 20Hz and 10kHz repetition rate with 5ns or 100ns pulse duration, respectively) to understand LA mechanisms of graphite surfaces with a deposited carbon layer (graphite tile from TEXTOR). The layer properties (thickness, thermal and optical properties, adhesion) were estimated by laser active pyrometer measurements. For a thick deposited layer (~30-50μm), the thermal model was applicable only to interpret LA thresholds rather than LA rates. In contrast to tokamak graphite [27], the LA rates calculated within the surface sublimation mechanism are rather small if compared with the experimental ones. Thus, it was concluded that for tokamak graphite and thick deposited carbon layers, LA mechanisms are qualitatively different. To explain the extremely high LA rates of a thick deposited carbon layer (if compared with those of tokamak graphite) which were observed experimentally in our studies, one may suggest a thermally induced mechanical disintegration (thermal shock sputtering) of a friable thick carbon deposited layer with a weak adhesion to the graphite substrate.

One may expect that the laser active pyrometry method may find its wider application in characterisation of other samples with a surface layer. For example, for a metal layer on a substrate of known properties, some layer features (layer thickness, adhesion) may be directly determined with pyrometer measurements.

ACKNOWLEDGEMENTS

This work was performed within the frames of the Euratom-CEA underlying technological program, tasks UT-S&E - LASER/DEC and FT-JW6-FT-3.30.

REFERENCES

[1]. I. Youle, A.A Haasz, Profiling with tritium imaging, Journal of Nuclear Materials **248** (1997)64.

[2]. G. Federici, R.A. Anderl, P. Andrew, J.N. Brooks, R.A. Causey, J.P. Coad, D. Cowgill, R.P. Doerner, A.A. Haasz, G. Janeschitz, W. Jacob, G.R. Longhurst, R. Nygren, A. Peacock, M.A. Pick, V. Philipps, J. Roth, C.H. Skinner, and W.R. Wampler, In-vessel tritium retention and removal in ITER, Journal of Nuclear Materials **266-269** (1999)14.

[3]. P. Andrew, D. Brennan, J.P. Coad, J. Ehrenberg, M. Gadeberg, A. Gibson, M. Groth, J. How, O.N. Jarvis, H. Jensen, R. Lsser, F. Marcus, R. Monk, P. Morgan, J. Orchard, A. Peacock, R. Pearce, M. Pick, A. Rossi, B. Schunke, M. Stamp, M. von Hellermann, D.L. Hillis, and J. Hogan, Tritium recycling and retention in JET, Journal of Nuclear Materials **266-269** (1999) 153.

[3] *For layer depth measurements, LIBS [24] may be suggested as a complementary method.*

[4]. M. Friedrich, W. Pilz, G. Sun, R. Behrisch, C. Garcia-Rosales, N. Bekris, and R.-D. Penzhon, Tritium depth profiling in carbon by accelerator mass spectrometry, Nuclear Instruments Methods B, **161-163** (2000) 216.

[5]. R.A. Causey, Hydrogen isotope retention and recycling in fusion plasma-facing components, Journal of Nuclear Materials **300** (2002) 91.

[6]. T. Tanabe, N. Bekris, P. Coad, C.H. Skinner, M. Glugda, and N. Miya, Tritium retention of plasma facing components in tokamaks, Journal of Nuclear Materials **313-316** (2003) 478.

[7]. C.H. Skinner, J.P. Coad, and G. Federici, Tritium Removal from Carbon Plasma Facing Components, Phys. Scr. T111 (2004) 92.

[8]. C.H. Skinner, H. Kugel, D. Mueller, B.L.Doyle, and W.R. Wampler, Tritium Removal by *CO* 2 Laser Heating, Proceedings of the 17 th IEEE/NPSS Symposium on Fusion Engineering (SOFE'97, 6-9 October 1997, San Diego, USA), vol.**1** (1998) pp.321-324.

[9]. C.H. Skinner, C.A. Gentile, A. Carpe, G. Guttadora, S. Langish, K.M. Young, W.M. Shu, and H. Nakamura, Tritium removal from codeposits on carbon tiles by a scanning laser, Journal of Nuclear Materials **301** (2002) 98.

[10]. C.H. Skinner, N. Bekris, J.P. Coad, C.A. Gentile, and M. Glugda, Tritium removal from JET and TFTR tiles by a scanning laser, Journal of Nuclear Materials **313-316** (2003) 496.

[11]. K.J. Gibson, G.F. Counsell, C. Curran, M.J. Forrest, M.J. Kay, and K.J. Watkins, The removal of co-deposited hydrocarbon films from plasma facing components using high-power pulsed flashlamp irradiation, Journal of Nuclear Materials **337-339** (2005) 565.

[12]. B. Emmoth, S. Khartsev, A. Pisarev, A. Grishin, U. Karlsson, A. Litnovsky, M. Rubel, and P. Wienhold, Fuel removal from bumper limiter tiles by using a pulsed excimer laser, Journal of Nuclear Materials **337-339** (2005) 639.

[13]. W. Shu, Y. Kawakubo, G.N. Luo, and M. Nishi, Removal of co-deposited layers by excimer lasers, Journal Nuclear Scientific Technology **40** (2003) 1019.

[14]. W.M. Shu, Y. Kawakubo, K. Masaki, and M.F. Nishi, Ablative removal of codeposits on JT-60 carbon tiles by an excimer laser, Journal of Nuclear Materials **313-316** (2003) 584.

[15]. F. Le Guern, C. Hubert, S. Mousset, E. Gautier, C. Blank, P. Wodling, and J.M. Weulersse, Laser ablation tests performed on TORE-SUPRA graphite samples, Journal of Nuclear Materials **335** (2004) 410.

[16]. T. Shibahara, Y. Sakawa, and T. Tanabe, Hydrogen release behavior from graphite under pulsed laser irradiation, Journal of Nuclear Materials **337-339** (2005) 654.

[17]. Y. Sakawa, T. Shibahara, K. Sato, and T. Tanabe, Pulsed laser ablation of hydrogen-implanted graphite target, Journal Plasma Fusion Results **7** (2006) 138.

[18]. Y. Sakawa, K. Sato, T. Shibahara, and T. Tanabe, Ablation of hydrogen-implanted graphite target using pulsed laser beam, Fusion Engineering Design **81** (2006) 381.

[19]. B. Schweer, A. Huber, G. Sergienko, V. Philipps, F. Irrek, H.G. Esser, V. Samm, M. Kempenaar, M. Stamp, C. Gowers, and D. Richards, Laser desorption of deuterium retained in re-deposited carbon layers at TEXTOR and JET, Journal of Nuclear Materials **337-339** (2005) 570.

[20]. A. Semerok, J.-M. Weulersse, F. Brygo, Ch. Lascoutouna, Ch. Hubert, F. Le Guern, and M. Tabarant, Studies on graphite surfaces detritiation by pulsed repetition rate nanosecond lasers, CEA report, NT-DPC/SCP/04-076-A (2004) pp.1-39.

[21]. A. Semerok, J.-M. Weulersse, F. Brygo, D. Farcage, C. Hubert, C. Lascoutouna, M. Geleoc, P. Wodling, H. Long, F. Champonnois, G. Brunel, G. Vimond, E. Lizon, V. Dauvois, V. Delanne, C. Grisolia, S. Fomichev, and M. Hashida, Studies on tokamak wall surfaces decontamination by pulsed repetition rate lasers, CEA report, NT-DPC/SCP/05-111-A (2005) pp.1-50.

[22]. A. Semerok, F. Brygo, S.V. Fomichev, F. Champonnois, J.-M. Weulersse, P.-Y. Thro, P. Fichet, and C. Grisolia, Laser detritiation and co-deposited layer characterisation for future ITER installation, The 9th European Nuclear Conference (Versailles, France, December 11 – 14, 2005), ENC'2005 Proceedings, 2005, p. 66.

[23]. A. Semerok, P.-Y. Thro, J.-M. Weulersse, S.V. Fomichev, F. Brygo, C. Grisolia, V. Philipps, and P. Coad, Laser methods development for in situ ITER walls detritiation and deposition layers characterization, 21st IAEA Fusion Energy Conference (FEC'2006), Chengdu, China, October 16–21, 2006, FEC'2006 Proceedings (Paper ID: IT/P1-15 on WEB-site'http://wwwnaweb.iaea.org/napc/physics/FEC/FEC2006/html/index.htm).

[24]. C. Grisolia, A. Semerok, J.-M. Weulersse, F. Le Guern, S.V. Fomichev, F. Brygo, P. Fichet, P.-Y. Thro, P. Coad, N. Bekris, M. Stamp, S. Rosanvallon, and G. Piazza, In situ Tokamak laser applications for detritiation and co-deposited layers studies, Journal of Nuclear Materials **363-365** (2007)1138.

[25]. B. Luk'yanchuk (editor), Laser Cleaning, World Scientific Publishing, Singapore, 2002.

[26]. C.H. Skiner, N. Bekris, J.P. Coad, C.A. Gentile, A. Hassanrin, R. Reiswig, and S. Willms, Thermal Response of Tritiated Codeposits from JET and TFTR to Transient Heat Pulses, Physica Scripta T103 (2003) 34.

[27]. A. Semerok, S.V. Fomichev, F. Brygo, J.-M. Weulersse, P.-Y. Thro, C. Grisolia, Heating and ablation of tokamak graphite by pulsed nanosecond Nd-YAG lasers, Journal Applied Physics **101** (2007) 084916.

[28]. A. Semerok, S.V. Fomichev, F. Brygo, and P.-Y. Thro, Laser heating of complex graphite surfaces by high repetition rate nanosecond pulses (comparative modelling and experimental studies), CEA report, NT-DPC/SCP/06-170-A (2006) pp.1 - 36.

[29]. F. Brygo, A. Semerok, R. Oltra, J.-M. Weulersse, and S. Fomichev, Laser heating and ablation at high repetition rate in thermal confinement regime, Applied Surface Science **252**, (2006) 8314.

[30]. Ch. L. Mantell, Carbon and Graphite Handbook, Interscience Publishers, New York, 1968.
[31]. I.S. Grigoryev, E.S. Meilikhov, A.A. Radzig (eds), Handbook of Physical Quantities, CRC Press, Roca Baton, FL, 1996.
[32]. E. N. Sobol, Phase Transformations and Ablation in Laser-Treated Solids, Wiley Interscience Publication, New York, 1995.
[33]. R. Kelly and A. Miotello, Comments on explosive mechanisms of laser sputtering, Applied Surface Science 96 - 98 (1996) 205.

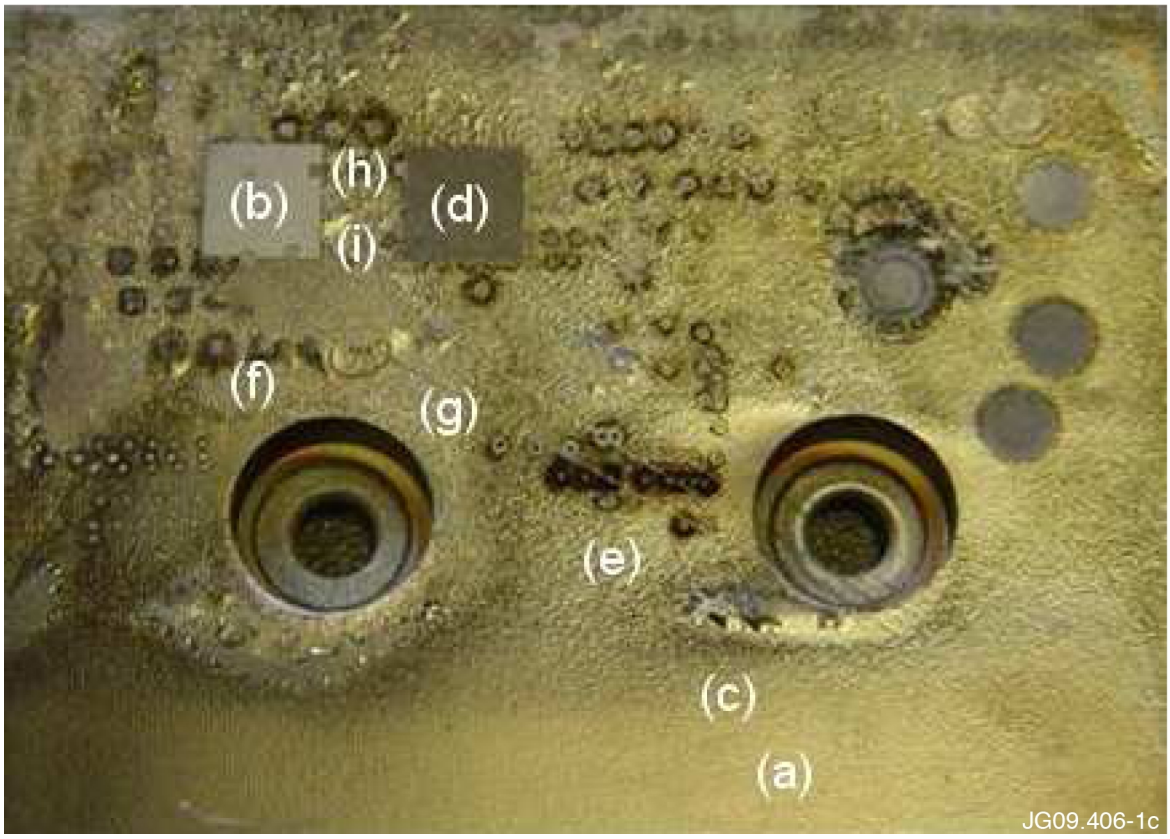

Figure 1: Plasma-facing surface of the TEXTOR graphite tile (ALT-II) with a deposited carbon layer of different thickness. Different tile zones under LH measurements are indicated as: (a) - without deposited layer, (b) - laser ablated area by 10 scans, (c) - a very thin deposited layer, (d) - laser ablated area by 1 scan, (e) - a thin deposited layer, (f) and (g) - a medium deposited layer, (h) and (i) - a thick deposited layer.

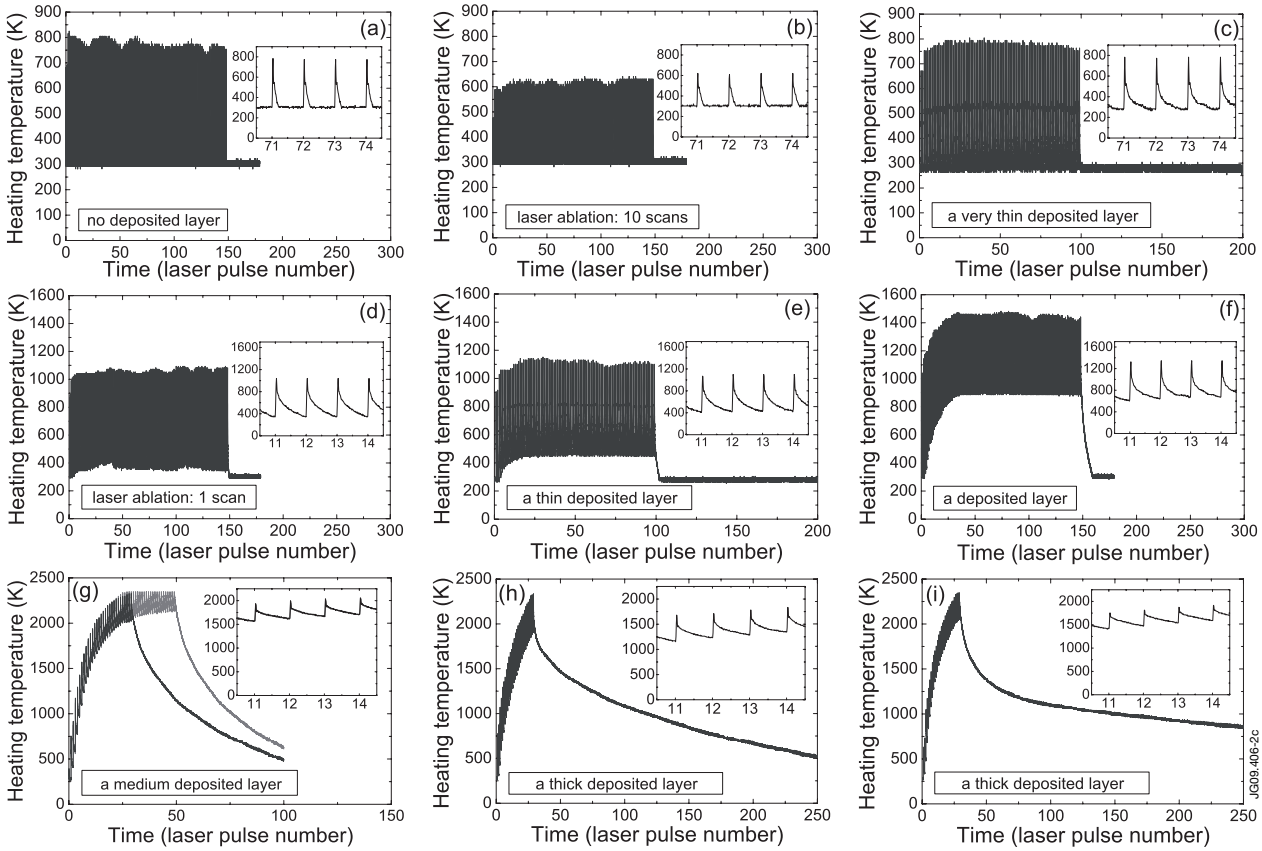

Figure 2: Panels (a) - (i) present the pyrometer measurements results on LH of plasma-facing surface of TEXTOR graphite tile on different tile zones in accordance with indications in Fig.1. The laser parameters are: $\lambda_L = 532nm$, $\nu_L = 10kHz$, $\tau_p = 100ns$, $E_p = 6mJ$, $F \cong 0.3\ J/cm^2$.

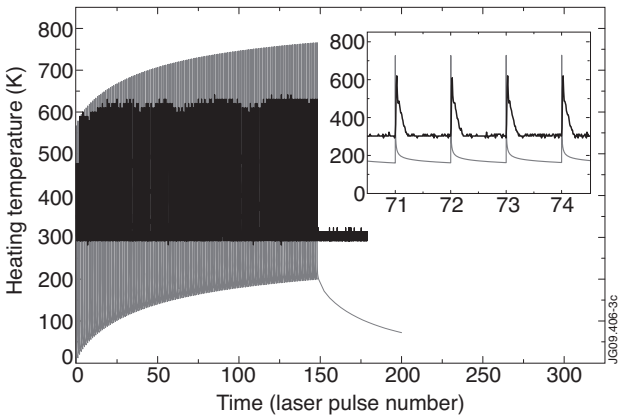

Figure 3: LH pyrometry results (black) for the completely ablated carbon layer zone on the TEXTOR graphite tile (case (b) on Figures 1 and 2) versus the theoretical calculations (gray) for LH of the graphite surface with the bulk graphite properties.

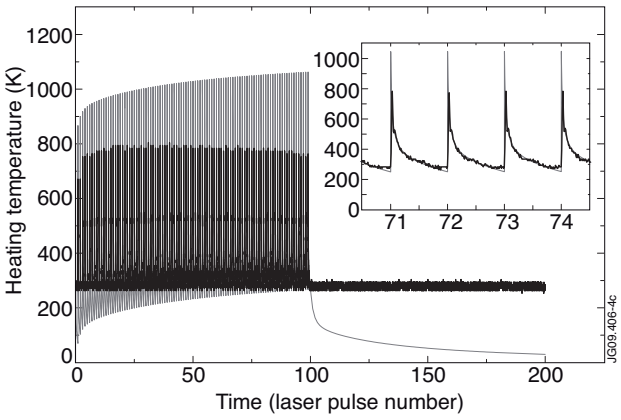

Figure 4: LH pyrometry results (black) for the TEXTOR graphite tile zone with a thin deposited carbon layer (panel (c) of Fig.2) versus the theoretical calculations (gray). The deposited layer properties are: $p_L = 0$, $d = 5\mu m$, $k_L = 0.7\ W/(m \cdot K)$, $h = 250kW/(m^2 \cdot K)$.

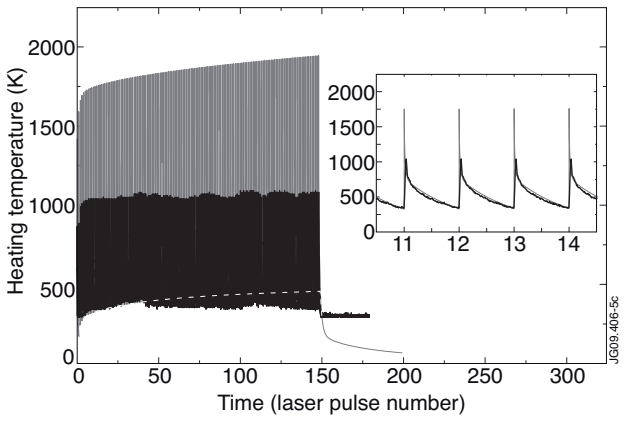

Figure 5: LH pyrometry results (black) for the partially ablated carbon layer on TEXTOR graphite tile (panel (d) of Fig.2) versus the theoretical calculations (gray). The residual carbon layer properties are: $p_L = 0$, $d = 1.7\mu m$, $k_L = 0.4W/(m\cdot K)$, $h = 60kW/(m^2\cdot K)$. White dash curve shows the envelope of the theoretical pre-heating temperatures.

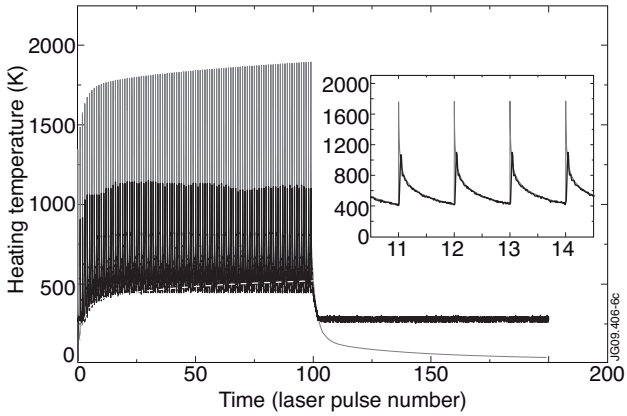

Figure 6: LH pyrometry results (black) for the TEXTOR graphite tile zone with the deposited carbon layer (panel (e) of Fig.2) versus the theoretical calculations (gray). The deposited layer properties are: $p_L = 0$, $d = 3.8\mu m$, $k_L = 0.2W(m\cdot K)$, $h=100\ kW/(m^2\cdot K)$. White dash curve shows the envelope of theoretical pre-heating temperatures.

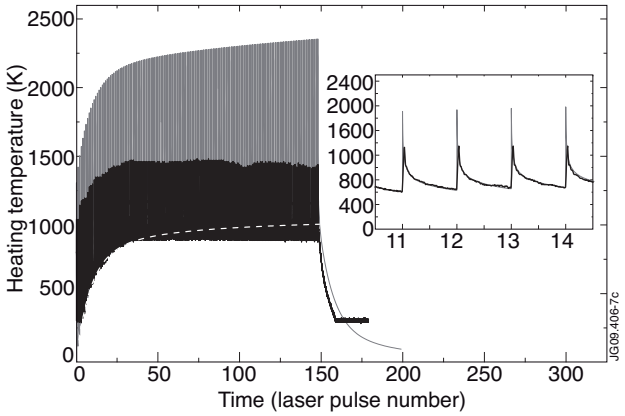

Figure 7: LH pyrometry results (black) for the TEXTOR graphite tile zone with the deposited carbon layer (panel (f) of Fig.2) versus the theoretical calculations (gray). The deposited layer properties are: $p_L = 0$, $d = 10\mu m$, $k_L = 0.4W(m\cdot K)$, $h = 60kW/(m^2\cdot K)$. White dash curve shows the envelope of theoretical pre-heating temperatures.

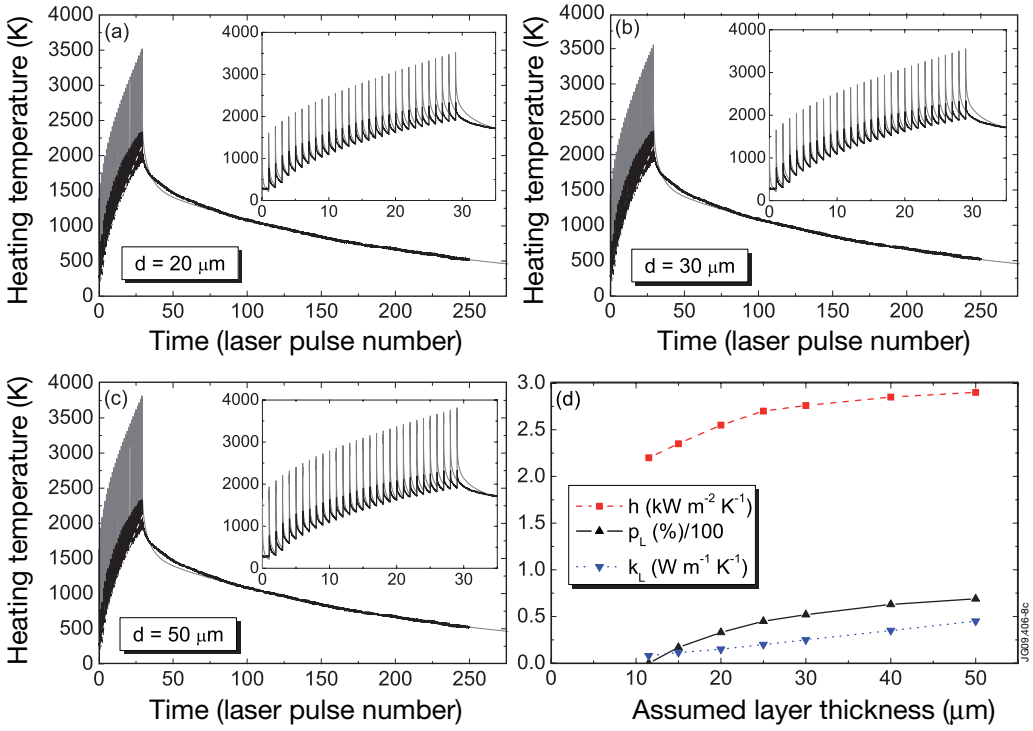

Figure 8. (Color online). Panels (a), (b) and (c): LH calculation results for three different assumed layer thickness d of 20, 30 and 50μm, respectively, versus LH pyrometry results for the zone on TEXTOR tile with a thick deposited carbon layer (panel (h) of Fig.2). White dash curve shows the envelope of theoretical pre-heating temperatures. Panel (d): dependences of three adjusting parameters p_L, k_L and h) on assumed layer thickness (calculated points and interpolated curves).

Figure 9: Panels (a), (b) and (c): LH calculation results for three different assumed layer thickness d of 20, 40 and 50μm, respectively, versus LH pyrometry results for the zone on TEXTOR tile with a thick deposited carbon layer (panel (i) of Fig.2). White dash curve shows the envelope of theoretical pre-heating temperatures. Panel (d): dependences of three adjusting parameters (p_L, k_L and h) on assumed layer thickness (calculated points and interpolated curves).

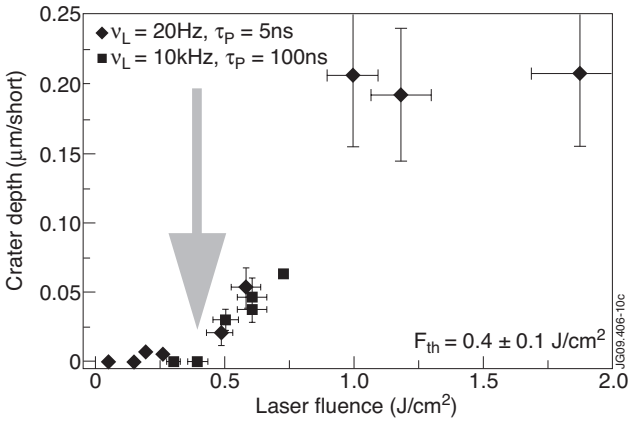

Figure 10: (Color online). Experimental crater depth (per one laser shot) versus laser fluence for a TEXTOR graphite tile with a thick deposited carbon layer for two different homogenized Nd-YAG laser beams with λ_L = 532nm. The thick line corresponds to the top theoretical limit of LA rate due to the surface sublimation mechanism.

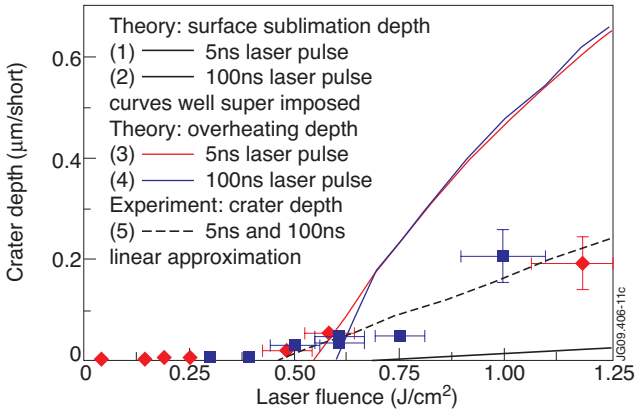

Figure 11: (Color online). Simulation results of the deposited layer LA within the framework of the Stefan-like sublimation model versus the experimental results of Fig.10.

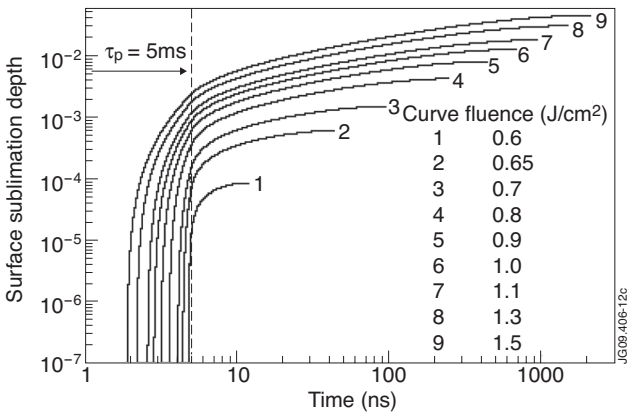

Figure 12: Calculated surface sublimation depth (in µm) of deposited carbon layer for 5ns laser pulse at different laser fluence as a function of time.

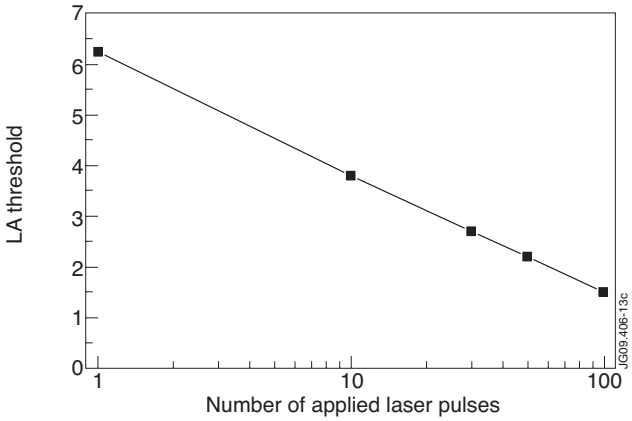

Figure 13: Theoretical dependence of LA threshold (J/cm^2) for a thick (40µm) deposited carbon layer with adjusting parameters of Fig.9 (d) versus the number of applied laser pulses of 100ns pulse duration and 10kHz repetition rate (calculated points and interpolated line).